Surface-spin magnetism of antiferromagnetic NiO in nanoparticle and bulk morphology

2009 J. Phys.: Condens. Matter 21 215302

(http://iopscience.iop.org/0953-8984/21/21/215302)

J. Phys.: Condens. Matter **21** (2009) 215302 (6pp) doi:10.1088/0953-8984/21/21/215302

Surface-spin magnetism of antiferromagnetic NiO in nanoparticle and bulk morphology

M Jagodič[1], Z Jagličić[1], A Jelen[2], Jin Bae Lee[3], Young-Min Kim[4], Hae Jin Kim[3] and J Dolinšek[2]

[1] Institute of Mathematics, Physics and Mechanics, University of Ljubljana, Jadranska 19, SI-1000 Ljubljana, Slovenia
[2] J Stefan Institute, University of Ljubljana, Jamova 39, SI-1000 Ljubljana, Slovenia
[3] Nano Material Team, Korea Basic Science Institute, Daejeon 305–806, Korea
[4] Division of Electron Microscopy Research, Korea Basic Science Institute, Daejeon 305–806, Korea

Received 24 February 2009
Published 30 April 2009
Online at stacks.iop.org/JPhysCM/21/215302

Abstract

The surface-spin magnetism of the antiferromagnetic (AFM) material NiO in nanoparticle and bulk morphology was investigated by magnetic measurements (temperature-dependent zero-field-cooled (zfc) and field-cooled (fc) dc susceptibility, ac susceptibility and zfc and fc hysteresis loops). We addressed the question of whether the multisublattice ordering of the uncompensated surface spins and the exchange bias (EB) effect are only present in the nanoparticles, originating from their high surface-to-volume ratio or if these surface phenomena are generally present in the AFM materials regardless of their bulky or nanoparticle morphology, but the effect is just too small to be detected experimentally in the bulk due to a very small surface magnetization. Performing experiments on the NiO nanoparticles of different sizes and bulk NiO grains, we show that coercivity enhancement and hysteresis loop shift in the fc experiments, considered to be the key experimental manifestations of multisublattice ordering and the EB effect, are true nanoscale phenomena only present in the nanoparticles and absent in the bulk.

(Some figures in this article are in colour only in the electronic version)

As suggested by Néel in 1961, small particles of an antiferromagnetic (AFM) material behave differently from the bulk AFM by exhibiting superparamagnetism and weak ferromagnetism (FM) [1], while the bulk AFM is magnetically compensated and has zero net magnetic moment in zero applied field. Reducing the size of the AFM particles to the nanoscale dimension, the surface-to-volume ratio becomes sufficiently large that the uncompensated spins at the surface can yield a detectable net magnetic moment. Within the Néel model [1], the permanent magnetic moments were attributed to uncompensated spins on the two sublattices. However, experiments on NiO AFM nanoparticles [2] have shown that the two-sublattice model cannot account for the anomalous magnetic properties, such as large magnetic moments, enhanced coercivity and hysteresis loop shift on the field axis of up to 10 kOe in field-cooled (fc) experiments. Numerical modeling of spin configurations in NiO nanoparticles suggested a new finite-size effect, where the reduced coordination of surface spins causes a fundamental change in the magnetic order throughout the particle, by creating multisublattice (eight-, six- or four-sublattice) spin ordering. The multisublattice ordering allows for higher net magnetic moments as compared to the two-sublattice model, as well as for a variety of reversal paths for the spins upon cycling the applied field, which results in simultaneous coercivity enhancement and loop shift in the fc experiments relative to the zero-field-cooled (zfc) case. The enhanced coercivity and loop shift are a consequence of the exchange bias (EB) phenomenon [3], where a FM or a spin-glass-like surface shell is exchange-coupled to the AFM core. A clear understanding of the mechanisms involved in EB is still lacking [4–7]. The EB effect has also been observed in other AFM nanoparticles

such as CoO [8], CuO [9, 10], Co_3O_4 [11], Cr_2O_3 [12] and ferritin [13].

While the multisublattice ordering of surface spins has been elaborated for the case of AFM nanoparticles, it remains an open question whether this kind of ordering is a consequence of nanodimensions of the particles due to their high surface-to-volume ratio (i.e. is it a true nanoeffect?) or whether it is a surface phenomenon generally present in the AFM materials regardless of their bulky or nanoparticle morphology. Bulk AFMs also contain surface layers of uncompensated spins due to reduced coordination, and there is no *a priori* reason against multisublattice ordering and the EB effect of the surface spins. Due to the low surface-to-volume ratio of the bulky samples, the effect could just be too small to be detected experimentally. In this paper we present magnetic measurements (temperature-dependent zfc and fc dc susceptibility, ac susceptibility, zfc and fc hysteresis loops) performed on the NiO nanoparticles of different dimensions, complemented by measurements on the high-purity bulk NiO AFM material. We show that the EB effect is only present for the material with nanoparticle morphology, whereas it is absent in the bulk. Our work complements previous studies of the magnetic properties of NiO AFM nanoparticles, which in the literature are described mostly as a superparamagnetic system [14–19], whereas some authors argue that the system already behaves as a spin glass at temperatures as high as 150 K [20].

Magnetic measurements were performed with a Quantum Design SQUID magnetometer operating in the temperature range between 400 and 2 K and in magnetic fields up to 50 kOe. The NiO nanoparticles were synthesized by procedures similar to those used by others [16, 20] and involve annealing $Ni(OH)_2$ gel at temperatures between 523 to 773 K to yield nanoparticles and nanorods of different sizes. Their dimensions were estimated from the transmission electron microscopy (TEM) images. The first samples were nanoparticles (figures 1(a) and (b)) with an average cross-dimension of 7.4 nm with a standard deviation $\sigma = 1.3$ nm (abbreviated in the following as the NP-7 sample), the second were larger nanoparticles (figure 1(c)) with an average cross-dimension of 25 nm and $\sigma = 10$ nm (NP-25) and the third were nanorods (figure 1(d)) with an average length of 86 nm with $\sigma = 31$ nm and diameter 14 nm with $\sigma = 2$ nm (NR). For the bulk NiO, we used a commercial Alfa Aesar high-purity powder product (Puratronic®, 99.998% grade). The bulky powder (figure 1(e)) consisted of microcrystallites with an average cross-dimension of 830 nm and $\sigma = 360$ nm. The crystalline morphology of the powder grains is evident from the scanning electron microscopy (SEM) image shown in figure 1(f), where it is observed that several single crystals are usually intergrown within one bulky particle.

The zfc and fc dc magnetic susceptibilities $\chi = M/H$ were measured between room temperature (RT) and 2 K in a magnetic field of 100 Oe and the data are displayed in figure 2(a). For all three kinds of nanodimension particles, the zfc–fc splitting (a signature of non-ergodicity and remanence of the spin system) is already observed at the highest investigated temperature of 300 K. According to literature reports, the zfc–fc splitting temperature of the NiO nanoparticles depends on the preparation conditions. The bifurcation temperature of about 300 K of our samples is similar to that of the NiO nanoparticles investigated in [18], whereas the nanoparticles investigated in [14, 16, 17, 20] show zfc–fc splitting at lower temperatures between 270 and 100 K (the lowest one being observed for the oleic-acid coated NiO nanoparticles [14]). The magnitudes of the fc susceptibility and the zfc–fc splitting of our samples increase with increasing particle size, being the smallest for the NP-7 nanoparticles, and increasing for the NP-25 nanoparticles towards the NR nanorods. This behavior is in contrast to the intuitive picture that larger surface-to-volume ratio of smaller particles should yield a larger fraction of uncompensated surface spins and hence larger magnetization and remanence (increasing as $1/D$, where D is the particle diameter). However, an identical relation to ours has been commonly found for NiO nanoparticles. Kodama *et al* [2] have reported that magnetic remanence, as a function of the particle diameter, exhibits a maximum for a diameter of about 200 nm, decreasing quite rapidly towards smaller diameters down to the 10 nm range and also decreasing (though less rapidly) for more bulky grains. A qualitatively similar dependence of the remanence on the particle diameter was also reported by Makhlouf *et al* [19], where the maximum was found for a particle diameter of about 30 nm. While the reason for the non-applicability of the $1/D$ law of the magnetization has still to be elaborated, it is worth mentioning that the $1/D$ dependence was predicted for spherical particles, whereas real particles of irregular shape, considerable surface corrugation and possible surface chemical inhomogeneity may not follow this consideration. In figure 2(a), the zfc and fc dc susceptibilities of the bulk NiO are displayed as well. The Néel temperature of the AFM transition in the bulk is $T_N = 523$ K, so that in our investigated temperature range below room temperature (RT) the system is in the AFM-compensated regime and the susceptibility is consequently very small. However, some remanence is also observed in the pure bulk NiO (figure 2(c)) below the zfc–fc bifurcation temperature of about 250 K. Due to the high purity of the bulk material, this remanence can be attributed to the uncompensated spins within the surface layer of the bulky grains.

The zfc susceptibilities of the three nanosamples show broad maxima at temperatures around 270 K. The ac susceptibility χ' measurements, performed in the ac magnetic field of amplitude $H_0 = 6.5$ Oe, at frequencies $\nu = 1$, 10, 100 and 1000 Hz and temperatures up to 345 K, reveal that the maxima are frequency-dependent, shifting to lower temperatures at lower frequencies (figures 3(a) and (b)). This feature is typical of a non-ergodic spin system, where spin fluctuations are frozen below the blocking temperature T_B, defined from the maximum in the ac susceptibility. The relatively broad and flat maxima reveal a distribution of blocking temperatures in each sample due to a distribution of particle sizes (this is more pronounced for the NR sample, figure 3(b)).

Inspecting carefully the temperature-dependent zfc and fc dc susceptibilities at low temperatures, we observe an

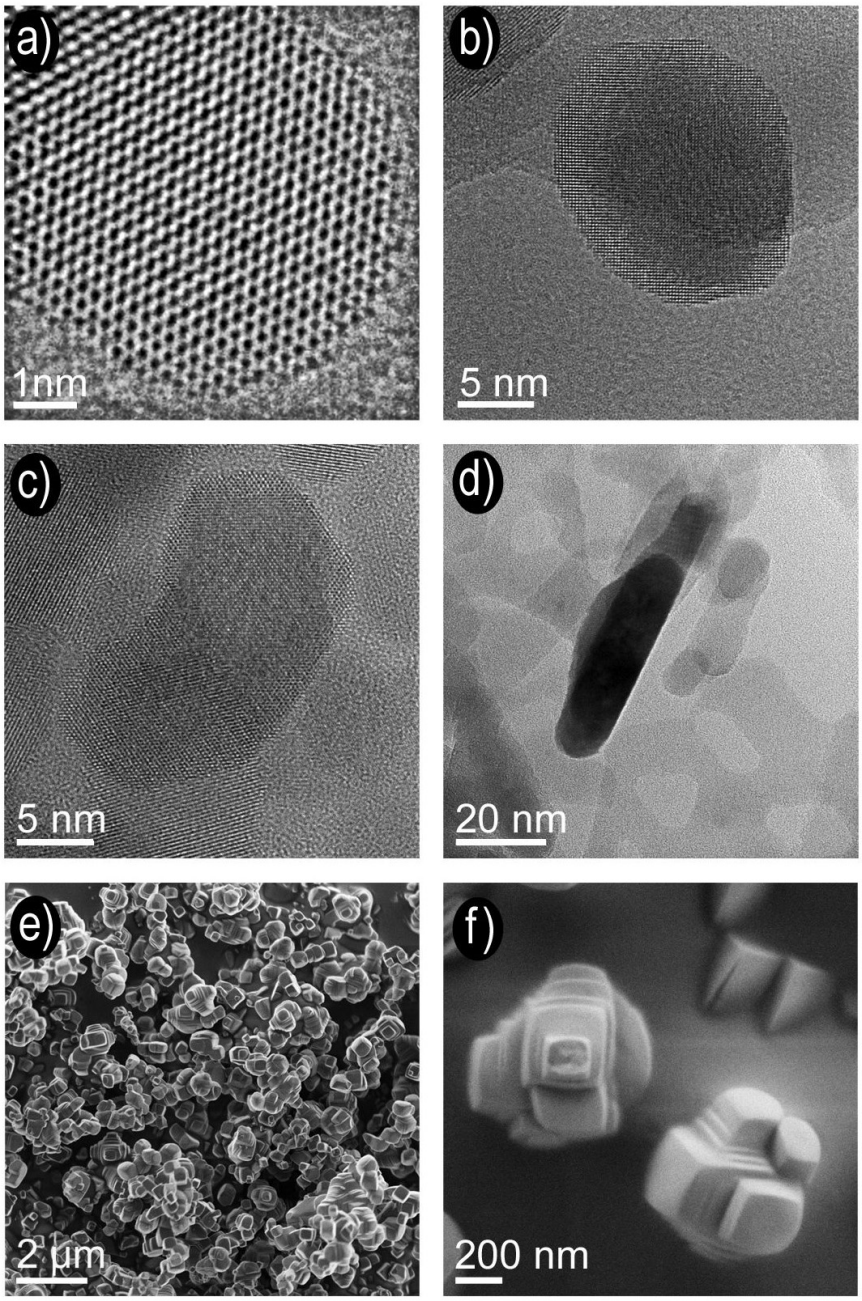

Figure 1. High-resolution HRTEM images of representative NiO nanoparticles and nanorods: (a) NP-7 sample, (b) and (c) NP-25 and (d) NR. The images were obtained using a JEOL JEM-ARM1300S high-voltage electron microscope (operated at 1250 kV) with 1.2 Å point-to-point resolution, so that atomic resolution of the nanoparticles is visible. In panel (e), a SEM secondary electron image of the bulk NiO commercial Alfa Aesar powder product (Puratronic®, 99.998% grade) is shown. The crystalline morphology of the powder grains is evident from panel (f).

additional feature at temperatures below 20 K. This is most clearly evident for the NP-7 sample (figure 2(b)), where the fc susceptibility increases rapidly below 20 K, whereas the zfc susceptibility exhibits another cusp below that temperature at about 14 K. The ac susceptibility χ' of this nanoparticle sample (figure 3(c)) reveals that the low-temperature cusp is frequency-dependent, shifting to lower temperatures at lower frequencies. The spin system obviously underwent a magnetic transition to a collective non-ergodic spin state. These are very likely FM domains at the surface of the nanoparticles. Similar anomalies in the zfc and fc dc susceptibilities below about 20 K, though somewhat smaller, can be noticed in figure 2(a) for the NP-27 and NR samples as well (indicated by arrows). Here it should be mentioned that the same type of anomalies can also be noticed in the susceptibility data of the NiO nanoparticles investigated by some other authors (e.g. the 'uncoated' sample in figure 1 of [18] and the 'uncoated-freeze-dried' sample in figure 3 of [14]), but no attention was given there to this effect. Compared to the bulk NiO (figure 2(c)), we observe, surprisingly, that an almost identical

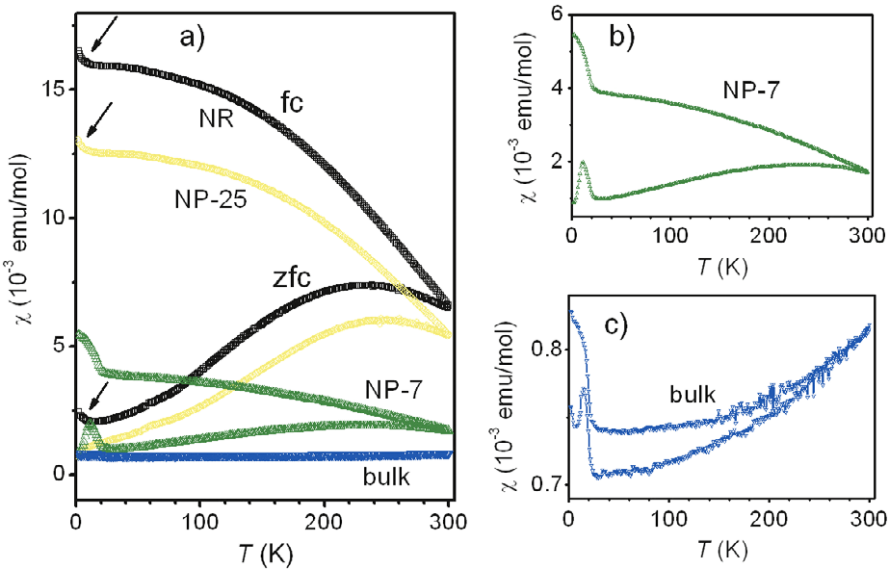

Figure 2. (a) The zfc and fc magnetic susceptibilities $\chi = M/H$ of the nanoparticles (samples NP-7 and NP-25), nanorods (NR) and the bulk NiO AFM powder material. In panels (b) and (c), the susceptibilities of the NP-7 and the bulk samples are displayed, respectively, on an expanded vertical scale, where the low-temperature transition to a collective magnetic state is evident in more detail. The arrows in panel (a) indicate that the low-temperature anomalies are also observed for the NP-25 and NR samples, though they are less pronounced.

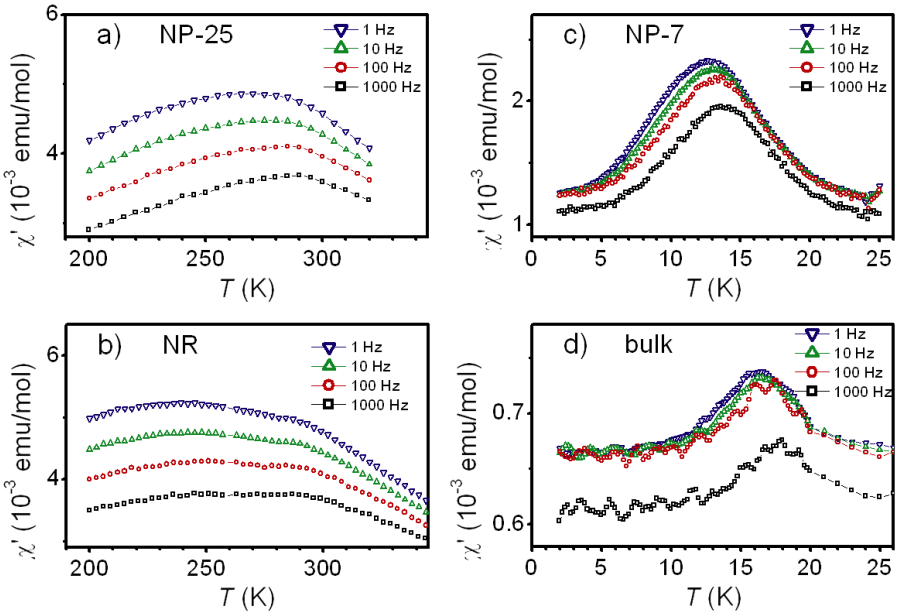

Figure 3. The real part of the ac susceptibility χ' at frequencies $\nu = 1$, 10, 100 and 1000 Hz. Panels (a) and (b) show the frequency-dependent cusp in χ' of the samples NP-25 and NR, respectively, in the high-temperature regime around room temperature. In panels (c) and (d), the frequency-dependent cusp in χ' is shown for the NP-7 and bulk samples at low temperatures below 25 K within the regime of the collective magnetic state.

low-temperature anomaly in the zfc and fc dc susceptibilities is also observed in the bulk material. The temperature (20 K) of the anomaly is the same as for the nanoparticles and the temperature dependence of the susceptibility is very similar to that of the NP-7 nanoparticles (the fc susceptibility jumps to a higher value, whereas the zfc susceptibility exhibits a cusp, which is frequency-dependent, as evidenced from the χ' measurements of the NiO bulk displayed in figure 3(d)). The main difference of the bulk NiO from the NP-7 sample is the magnitude of the dc susceptibility change, which in the bulk is about 15-times smaller compared to NP-7. The appearance of the collective magnetic state below 20 K is thus not a consequence of the nanodimensions of the particles and hence is not a nanoeffect—it is equally observed in the nanoparticles and in the bulky grains of the powder material. This is another indication that bulky AFM grains also contain uncompensated spins at the surface, some of which undergo a transition to a collective magnetic state (very likely localized FM domains) at low temperature in the same way as the uncompensated surface spins of the nanoparticles. The reason

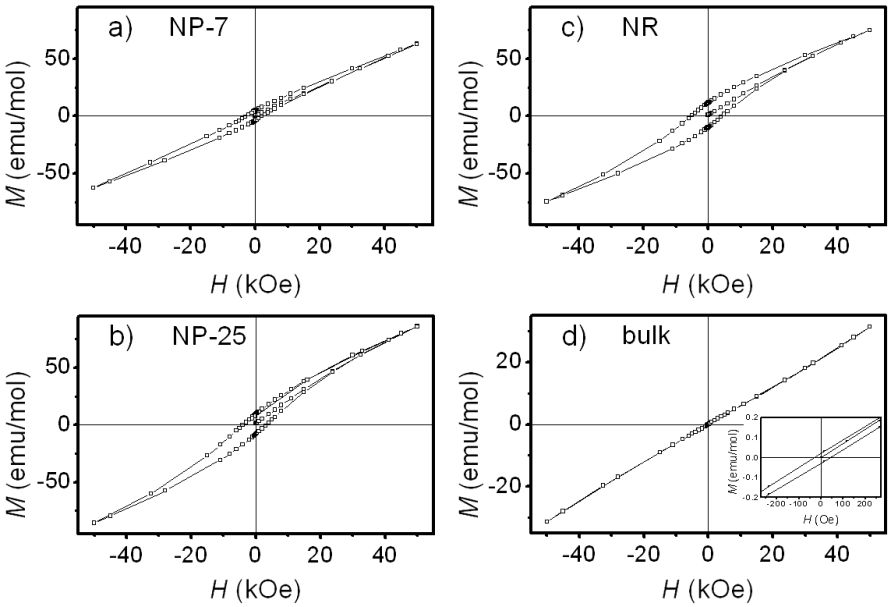

Figure 4. The zfc hysteresis loops at 2 K of (a) NP-7, (b) NP-25, (c) NR and (d) the bulk NiO sample. For the bulk sample, the loop expanded around $H = 0$ is shown as an inset. Note that the vertical M axis is the same for the three nanodimension samples, whereas it is expanded for the bulk sample.

that the weak surface-spin magnetism of the bulk NiO could be experimentally observed is due to the fact that the core spins of the bulky grains are almost perfectly AFM compensated, so that their magnetization is practically zero and the small magnetization of the surface spins becomes observable with a high-sensitivity SQUID magnetometer. The appearance of the low-temperature collective magnetic state reveals that at least a fraction of the surface spins are strongly exchange-coupled, regardless of the nanoparticle or bulky morphology of the material.

The $M(H)$ hysteresis loops were investigated in the fields up to 50 kOe under both zfc and fc conditions. The zfc loops at 2 K are displayed in figure 4. The loops of the three nanodimension particles NP-7 (figure 4(a)), NP-25 (figure 4(b)) and NR (figure 4(c)) are typically AFM, remaining open up to 50 kOe (recall that a typical FM loop saturates quite rapidly for much lower fields of a few kOe) and being superposed onto the field-linear AFM contribution. As perfectly compensated AFMs do not show hysteresis, this confirms that the magnetic moments of the nanoparticles originate from the uncompensated surface spins. The zfc coercive field H_c^{zfc} increases with increasing particle size, amounting at 2 K to 2400 Oe for NP-7, 3500 Oe for NP-25 and 4500 Oe for NR. This trend is in agreement with the zfc–fc splitting of the dc susceptibility (that reflects the remanence of the spin system), which increases in the same order of samples. In figure 4(d), the $M(H)$ data of the bulk NiO are shown, exhibiting a linear M–H relation typical of a compensated AFM. However, a small hysteresis with $H_c^{zfc} \approx 40$ Oe at 2 K is also observed in the bulk material (inset in figure 4(d)), in agreement with the observed zfc–fc splitting of the dc susceptibility of the bulk sample (figure 2(c)). This is another experimental confirmation that uncompensated spins exist at the surface of the bulky grains as well.

The fc hysteresis loops were measured by cooling the samples from RT in a field of 20 kOe. In figure 5(a), the zfc and fc loops at 2 K of the NP-7 sample are shown on the same graph. The coercivity of the fc loop is enhanced by a factor of 2 with respect to the zfc case and the loop is strongly shifted by an amount approximately equal to the value of the coercivity. The temperature-dependent zfc and fc coercive fields, H_c^{zfc} and H_c^{fc}, and the exchange bias field H_E (the shift on the field axis) are displayed in figure 5(b). Since H_E is negative, its absolute value $|H_E|$ is shown. H_c^{zfc} does not show a pronounced temperature dependence below 100 K, whereas H_c^{fc} and H_E both show quite a strong temperature dependence, but without a pronounced anomaly in the vicinity of the low-temperature transition at 20 K (inset in figure 5(b)). Here it is worth mentioning that magnetic properties are complex functions of the particles' net moments, sizes, morphologies and crystal orientations, so that a quantitative analysis of the shifted loops and the associated H_c^{fc} and H_E parameters is a difficult task, involving modeling the distributions of these properties, and is beyond our capabilities. The zfc and fc hysteresis loops at 2 K of the bulk NiO, expanded around $H = 0$, are shown in figure 5(c). To within 10 Oe uncertainty, the fc loop obtained by cooling in 20 kOe does not show any coercivity enhancement or shift on the field axis with respect to the zfc loop. Since the enhanced coercivity and loop shift are considered to be the key experimental manifestations of the multisublattice surface-spin ordering and the EB effect, their presence in the nanoparticles and absence in the bulk suggests that these effects are true nanoscale phenomena, originating from the large surface-to-volume ratio of the AFM nanoparticles.

To summarize, we have addressed the question of whether the multisublattice ordering of the uncompensated surface spins in AFMs and the EB effect are true nanoscale

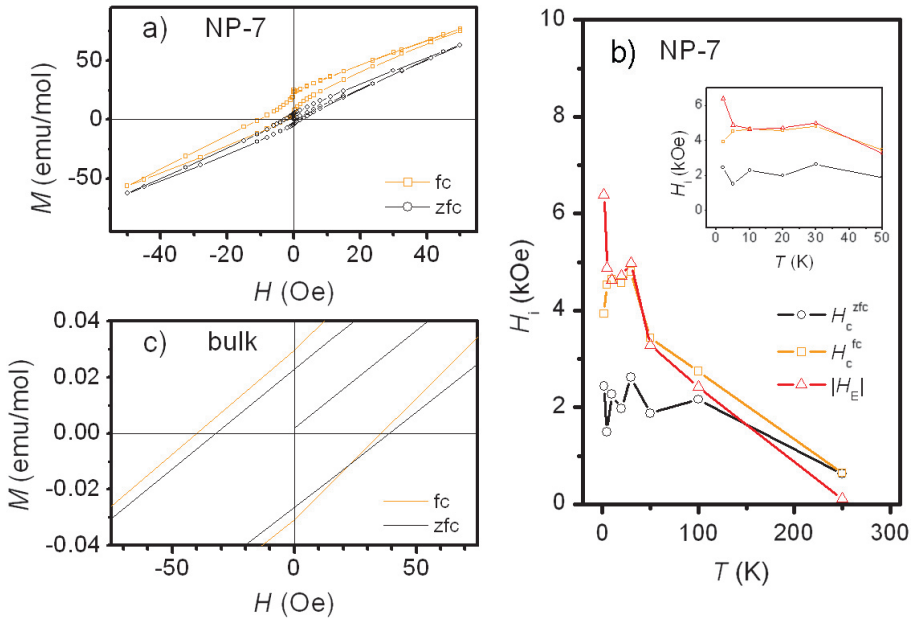

Figure 5. (a) The zfc and fc (after cooling in 20 kOe) hysteresis loops at 2 K of sample NP-7. In (b), the zfc and fc coercive fields H_c^{zfc} and H_c^{fc} and the (absolute) exchange bias field $|H_E|$ of sample NP-7, as a function of temperature, are shown. The inset shows an expanded portion of the graph below 50 K. Lines connect the points. (c) The zfc and fc loops of the NiO bulk on an expanded scale around $H = 0$.

phenomena, originating from the high surface-to-volume ratio of the nanoparticles, or if these surface phenomena are generally present in AFM materials regardless of their bulky or nanoparticle morphology, but the effect is just too small to be detected experimentally in the bulk due to a very small surface magnetization. Magnetic measurements were performed on NiO nanoparticles of different sizes, complemented by measurements on high-purity bulk NiO grains. The AFM-type zfc hysteresis loops confirm that uncompensated surface spins are present in both morphologies of the material. The zfc–fc susceptibility splitting and the frequency-dependent maxima in the ac susceptibility demonstrate that the spin system is non-ergodic below RT. The low-temperature transition at 20 K to a collective magnetic state, very likely FM surface domains, was equally found in the nanoparticles and in the bulk, demonstrating that at least a fraction of the surface spins are strongly coupled by the Ni–Ni superexchange interaction. The basic difference between the nanoparticles and the bulk is evident by comparing the zfc and fc hysteresis loops. While the fc loops of the nanoparticles show large coercivity enhancement and strong loop shift on the field axis, the fc loop of the bulk is not affected by the employed field of 20 kOe. This demonstrates that the multisublattice magnetic ordering of the uncompensated surface spins and the EB effect are true nanoscale phenomena related to the nanoparticle morphology of the AFM material. As the EB phenomenon plays a crucial role in spin-valve devices [4, 6, 21], application of the NiO (or other AFM) nanoparticles in spintronic devices is straightforward.

Acknowledgment

This work was supported by the Frontier Research Laboratory Program at the Korea Basic Science Institute.

References

[1] Néel L 1962 *Low Temperature Physics* ed C Dewitt, B Dreyfus and P D de Gennes (New York: Gordon and Breach) p 413
[2] Kodama R H, Makhlouf S A and Berkowitz A E 1997 *Phys. Rev. Lett.* **79** 1393
[3] Meiklejohn W P and Bean C P 1956 *Phys. Rev.* **102** 1413
[4] Nogués J and Schuller I K 1999 *J. Magn. Magn. Mater.* **192** 203
[5] Nogués J, Sort J, Langlais V, Skumryev V, Suriñach S, Muñoz J S and Baró M D 2005 *Phys. Rep.* **422** 65
[6] Berkowicz A E and Takano K 1999 *J. Magn. Magn. Mater.* **200** 552
[7] Stiles M D and McMichael R D 2001 *Phys. Rev.* B **63** 064405
[8] Zhang L, Xue D and Gao C 2003 *J. Magn. Magn. Mater.* **267** 111
[9] Punnoose A and Seehra M S 2002 *J. Appl. Phys.* **91** 7766
[10] Seehra M S and Punnoose A 2003 *Solid State Commun.* **128** 299
[11] Makhlouf S A 2002 *J. Magn. Magn. Mater.* **246** 184
[12] Makhlouf S A 2004 *J. Magn. Magn. Mater.* **272** 1530
[13] Makhlouf S A, Parker F T and Berkowitz A E 1997 *Phys. Rev.* B **55** R14717
[14] Bødker F, Hansen M F, Bender Koch C and Mørup S 2000 *J. Magn. Magn. Mater.* **221** 32
[15] Abdul Khadar M, Biju V and Inoue A 2003 *Mater. Res. Bull.* **38** 1341
[16] Seehra M S, Dutta P, Shim H and Manivannan A 2004 *Solid State Commun.* **129** 721
[17] Seehra M S, Shim H, Dutta P and Manivannan A 2005 *J. Appl. Phys.* **97** 10J509
[18] Shim H, Dutta P, Seehra M S and Bonevich J 2008 *Solid State Commun.* **145** 192
[19] Makhlouf S A, Al-Attar H and Kodama R H 2008 *Solid State Commun.* **145** 1
[20] Tiwari S D and Rajeev K P 2005 *Phys. Rev.* B **72** 104433
[21] Fert A and Piraux L 1999 *J. Magn. Magn. Mater.* **240** 338